

Metal Membranes with Hierarchically Organized Nanotube Arrays

W. Lee,* M. Alexe, K. Nielsch, and U. Gösele

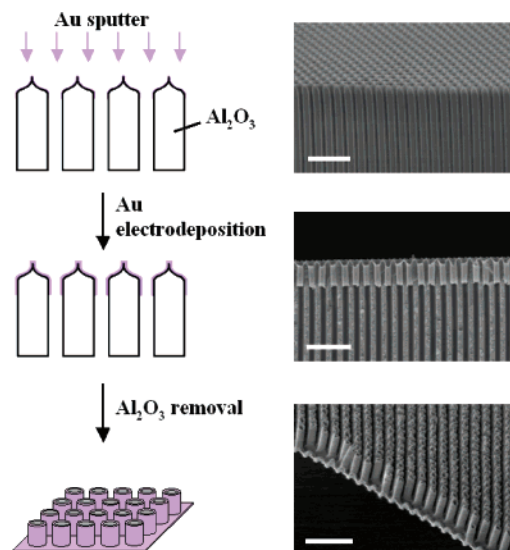
Max Planck Institute of Microstructure Physics,
Weinberg 2, D-06120 Halle, Germany

Received March 3, 2005

Revised Manuscript Received May 14, 2005

Two-dimensional (2-D) periodic arrays of metal or semiconductor nanostructures have attracted a lot of research interest due to their potential applications, e.g., for high-density magnetic media,¹ electronic/optoelectronic devices,² or bio-sensors.³ The most convenient and economic approach for the large-scale fabrication of periodic nanostructures in the submicrometer range is the shadow mask technique. This approach involves naturally occurring self-organized structures as a shadow mask in reactive ion-beam etching (RIE),⁴ X-ray lithography,⁵ or sputter deposition.⁶ Self-assembled microbeads (such as polystyrene or SiO₂) and nanoporous anodic aluminum oxide (AAO) have been used as a mask for generating large-area hexagonal arrays of nanostructured semiconductors,^{6a} metals,^{6b–d} and oxides.⁷ In fact, several groups have demonstrated that thin AAO membranes can be used as sputter masks for obtaining metal nanodot arrays with short-range ordering. However, this approach has two major disadvantages for practical applications. (1) The preparation of the through-hole membrane requires the removal of the barrier oxide layer by chemical etching. This step is inevitably accompanied by a significant enlargement of the pore diameter (D_p) from an initial pore diameter from $D_p \sim 0.3D_{\text{int}}$ up to $D_p > 0.8D_{\text{int}}$ (D_{int} = the interpore distance).⁸ Therefore previous attempts have failed on the tunability of the dot diameter (D_{Dot}). Nanodot arrays whose $D_{\text{Dot}} \leq D_p \approx 0.3D_{\text{int}}$ (D_p of an as-prepared alumina membrane) could not be fabricated. (2) The extremely brittle, ultrathin, and transparent nature of the AAO membrane

Scheme 1. Schematic Outline of the Experimental Procedure Used to Fabricate Free-Standing Au Nanotube Membrane^a



^a SEM micrographs of the corresponding sample structure are presented on the right side (scale bar = 2 μm).

makes it difficult to transfer oxide membranes larger than a few mm² onto an appropriate substrate. Due to the stiffness of the AAO membranes, large areas of the oxide shadow masks are not in contact with the substrate and voids with an area size of a few mm² occur between the membrane and the substrate surface which leads to an inhomogeneous pattern transfer. Alternatively, Pearson and Tonucci have used metallic antidot arrays as sputter masks for the fabrication of nanodot arrays.⁹ They obtained the metallic masks with a thickness of 40 nm by means of sputter deposition onto nanochannel glass (NCG) materials. Since the glass masters are based on optical fibers for telecommunication applications, the size of these metallic membranes is limited to one mm². Here we report a novel method for fabricating hierarchically organized arrays of Au nanotubes in the form of membranes, which can be used as shadow masks for generating spatially well-resolved 2-D periodic dot array with a perfect arrangement on a cm² scale.

Electrochemical deposition is used to replicate a master pattern of perfectly ordered AAO membrane based on imprint lithography.¹⁰ The fabrication process is outlined in Scheme 1. A thin metallic gold film was sputtered onto the surface of the AAO template at a deposition rate of 1 nm/min for 3 min. This process resulted in a thin conducting metal layer on the top part of the inner nanochannel surface as well as on the top surface of the AAO template. Subsequent electrochemical deposition (current density $\approx 1.5 \text{ mA/cm}^2$) of Au from a commercial electrolyte (Umicore, Auruna 5000) homogeneously thickens the metal layer, resulting in a tubular metallic nanostructure inside the alumina nano-

* To whom correspondence should be addressed. E-mail: woolee@mpi-halle.de.

- (1) (a) Liu, X.; Fu, L.; Hong, S.; Dravid, V. P.; Mirkin, C. A. *Adv. Mater.* **2002**, *14*, 231. (b) Koike, K.; Matsuyama, H.; Hirayama, Y.; Tanahashi, K.; Kanemura, T.; Kitakami, O.; Shimada, Y. *Appl. Phys. Lett.* **2001**, *78*, 784.
- (2) (a) Jacobs, H. O.; Whitesides, G. M. *Science* **2001**, *291*, 1763. (b) Ho, P. K. H.; Thomas, D. S.; Friend, R. H.; Tessler, N. *Science* **1999**, *285*, 233.
- (3) (a) Renault, J. P.; Bernard, A.; Juncker, D.; Michel, B.; Bosshard, H. R.; Delamarche, E. *Angew. Chem., Int. Ed.* **2002**, *41*, 2320. (b) Pirrung, M. C. *Angew. Chem., Int. Ed.* **2002**, *41*, 1276.
- (4) (a) Liang, J.; Chik, H.; Yin, A.; Xu, J. *J. Appl. Phys.* **2002**, *91*, 2544. (b) Crouse, D.; Lo, Y.-H.; Miller, A. E.; Crouse, M. *Appl. Phys. Lett.* **2000**, *76*, 49.
- (5) Knaack, S. A.; Eddington, J.; Leonard, Q.; Cerrina, F.; Onellion, M. *Appl. Phys. Lett.* **2004**, *84*, 3388.
- (6) (a) Bullen, H. A.; Garrett, S. J. *Nano Lett.* **2002**, *2*, 739. (b) Masuda, H.; Yasui, K.; Nishio, K. *Adv. Mater.* **2000**, *12*, 1031. (c) Masuda, H.; Yasui, K.; Sakamoto, Y.; Nakao, M.; Tamamura, T.; Nishio, K. *Jpn. J. Appl. Phys.* **2001**, *40*, L1267. (d) Sander, M. S.; Tan, L.-S. *Adv. Funct. Mater.* **2003**, *13*, 393.
- (7) Ma, W.; Harnagea, C.; Hesse, D.; Gösele, U. *Appl. Phys. Lett.* **2003**, *83*, 3770.
- (8) Nielsch, K.; Choi, J.; Schwirn, K.; Wehrspohn, R. B.; Gösele, U. *Nano Lett.* **2002**, *2*, 677.

(9) Pearson, D. H.; Tonucci, R. J. *Science* **1995**, *270*, 68.

(10) Choi, J.; Nielsch, K.; Reiche, M.; Wehrspohn, R. B.; Gösele, U. *J. Vac. Sci. Technol. B* **2003**, *21*, 763.

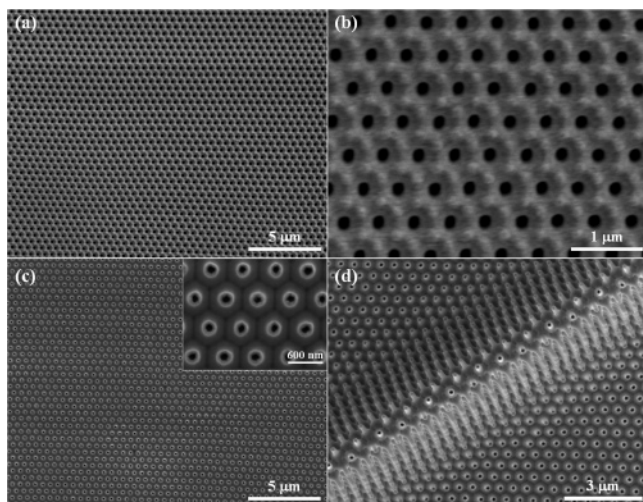


Figure 1. Representative SEM images of the Au nanotube membranes: (a) front surface view; (b) magnified view of (a); (c) back surface view with a magnified image in inset; and (d) back surface view of a bent membrane forming a ridge along the diagonal illustrating the 3-D structure of the membrane.

channels. The resulting gold membrane was floated on the surface of an etching solution (30 wt. % H_3PO_4 , 80 °C) to release it from the alumina template. Subsequently solution

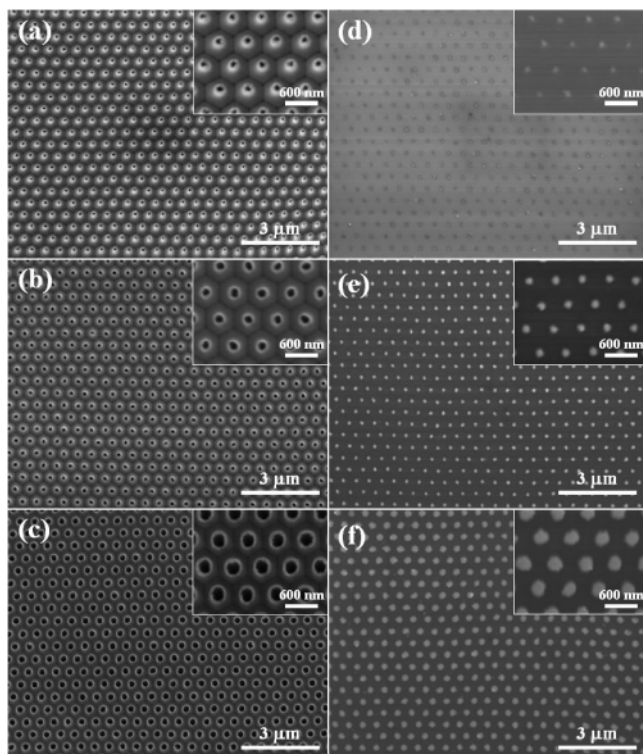


Figure 2. (a–c) SEM images of Au nanotube membranes fabricated from nanoporous AAO templates with different pore diameters (182, 222, and 326 nm for a, b, and c, respectively). Electrodeposition was carried out at a current density of 1.5 mA/cm² for 50 s at 17 °C. (d–f) SEM images of 2-D arrays of Pt nanodots sputtered on Si substrate by using respective membranes a–c. The high magnification views of each micrograph are presented as inset.

neutralization was carried out by replacing the etching solution (H_3PO_4) with deionized water. The Au nanotube membrane remained floating on the surface of the etching solution and could be easily transferred onto any substrate.

The two different sides of the Au nanotube membranes are shown in Figure 1. The front side (a) is characterized by a close-packed hexagonal arrangement of nanopores with a center-to-center distance of 500 nm, in which each pore is surrounded by six distinct bumps (b). This unique surface topography is similar to that of the as-anodized AAO template, revealing homogeneous electrodeposition of Au on the pre-deposited conducting metal layer. The backside image of the Au nanotube membrane shows a uniform array of interconnected Au nanotubes (c and d). Figure 1c shows a top view of the Au nanotube arrays, illustrating the open ends of the individual nanotubes. It should be noted that the channel diameter of the porous alumina template determines the outer tube diameter of the metal nanotube membrane. Meanwhile, the electrodeposition time determines the inner tube diameter of the resulting nanotubes (see Supporting Information). Accordingly, the fabrication of metal nanotube membranes with different tube diameters can be realized by using AAO templates with different channel diameters and/or by varying the electrochemical deposition time. As demonstrated in Figure 2a–c, we successfully fabricated Au nanotube membranes with different inner tube diameters (average diameter = 83 nm ($0.16D_{\text{int}}$), 126 nm ($0.25D_{\text{int}}$), and 230 nm ($0.46D_{\text{int}}$) for a–c, respectively) from nanoporous AAO templates by taking advantage of the easy control over the channel diameters via wet-chemical etching of AAO. The fabricated Au nanotube membranes were used as shadow masks for generating extended 2-D arrays (typically 1 cm²) of metal nanodots via sputter deposition.¹¹ Figure 2d–f show typical SEM images of Pt nanodot arrays sputtered on a silicon substrate using the Au nanotube membranes shown in Figure 2a–c as shadow masks. As evident from the presented SEM images, each nanodot is spatially well resolved with perfect hexagonal arrangement. According to SEM analyses, the average diameter of Pt nanodots of each sample is in good agreement with the inner-tube diameter of the respective shadow masks. Since the thickness of Pt is much smaller than the inner-tube diameter of Au nanotube, the deposited Pt nanodots have disklike structures. The inner-tube diameter of the gold nanotubes can be varied over a large range. Therefore, the size of the deposited metallic nanodots can be tuned over the same size range, irrespective of the interdot distances. It is expected that such a unique capability of tailoring the dot sizes independent of the interdot distance will enable us to, e.g., systematically investigate the magnetic coupling between neighboring magnetic nanodots. Due to the nanotube architecture and the thin film interconnections between the tubes, the gold membranes are extremely flexible and show an excellent adjustment to the substrate topography. In comparison with photoresist-based nanopatterning, where organic solvents are required for the lift-off processes, the present process is free of cross-contaminations or structural failures, which is often an important issue when the solvents are not compatible with the nanodot material and the substrate. In addition, the gold masks are very suitable for lift-off processes, where high temperatures are required for the substrate during deposition, or for nanopatterning within ultrahigh vacuum systems because metal masks have much better thermal stability

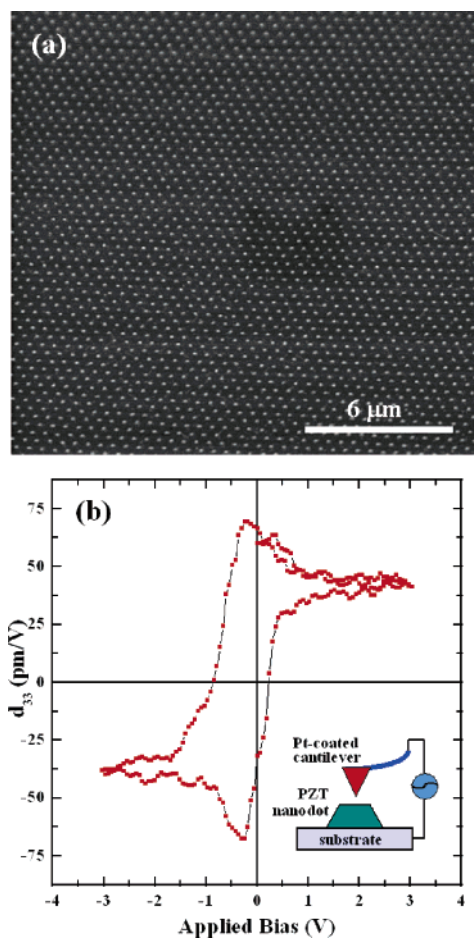


Figure 3. (a) SEM image of a large array of ferroelectric $\text{Pb}(\text{Zr}_{0.40}\text{Ti}_{0.60})\text{O}_3$ (PZT) nanodots on a Nb-doped SrTiO_3 single-crystal substrate with (111)-orientation, together with (b) a typical piezoelectric hysteresis loop obtained from a single PZT nanodot. Schematic of a piezoresponse-scanning force microscopy (PFM) measurement is presented as an inset in (b).

compared to most polymeric photoresists. These merits make the present technique very competitive with e-beam lithography, if large area periodic patterns are to be fabricated.

For more practical applications, we have demonstrated the fabrication of ferroelectric nanodot arrays that are suitable for nonvolatile data storage media with ultrahigh density. Figure 3a shows a SEM image of a vast array of ferroelectric $\text{Pb}(\text{Zr}_{0.40}\text{Ti}_{0.60})\text{O}_3$ (PZT) nanostructures on a Nb-doped SrTiO_3 single-crystal substrate with (100)-orientation. The ferroelectric nanodot arrays were fabricated by pulsed laser deposition (PLD) of PZT using an Au nanotube membrane as shadow mask. A typical ferroelectric hysteresis curve measured from a single ferroelectric nanodot is presented in Figure 3b. The dots show well-developed ferroelectric hysteresis curves as determined by piezoresponse-scanning force microscopy (PFM) with a coercive voltage of about

1 V and an effective remanent piezoelectric constant of 60 pm/V, which is about half of the values usually obtained on thick films.^{12,13} These observations demonstrate that each PZT nanodot has good switching properties and can act as a memory element in nonvolatile ferroelectric random access memory (NV-FRAM) devices.

Our approach is not limited to anodic alumina and provides a generalized way for the replication of metal nanotube membranes from various patterned substrates. We have successfully replicated, e.g., patterns from macroporous silicon with 2- μm interpore distance (see Supporting Information). Moreover, the nanofabrication method can be readily extended to other metallic or even semiconducting materials that can be electrodeposited. Therefore, it is expected that the metal nanotube membranes can have potential applications in near-field optics, nanophotonics, plasmonic nanolithography, nanohole-enhanced Raman spectroscopy, and biological sensing, by taking advantage of both the extraordinary optical properties (preliminary optical data, see Supporting Information) expected from subwavelength metal hole arrays¹⁴ and the ease of modification of metal surfaces with various functional molecules (e.g., proteins, DNAs, dyes) via self-assembly.

Acknowledgment. Financial support from the German Federal Ministry for Education and Research (BMBF, Project 03N8701) and the Volkswagen Foundation (Project I/80897) is greatly acknowledged. We thank Dr. D. Hesse for helpful discussions on ferroelectric nanostructures and S. Matthias for macroporous silicon sample preparation.

Supporting Information Available: Experimental details on the fabrication of nanoporous anodic aluminum oxide (AAO) and ferroelectric $\text{Pb}(\text{Zr}_{0.40}\text{Ti}_{0.60})\text{O}_3$ (PZT) nanodot arrays, details on piezoresponse-scanning force microscopy (PFM) measurements on PZT nanodots, SEM images of Au nanotube membranes showing the effect of electrodeposition time on the inner-tube diameter, SEM images of Au nanotube membranes replicated from patterned Si, and transmission spectra of Au nanotube membranes. This material is available free of charge via the Internet at <http://pubs.acs.org>.

CM050480Z

- (11) In sputter deposition experiments, the nanotube side of the Au membranes was in contact with the substrate.
- (12) Bolten, D.; Böttger, U.; Waser, R. *J. Eur. Ceram. Soc.* **2004**, *24*, 725.
- (13) The observed piezoelectric coefficient being smaller than those of thin films, as well as the shift of the hysteresis loop towards negative voltages, can be explained as extrinsic size effects originating on one side from the relatively low thickness and on the other side from the strong asymmetry in the bottom and top electrodes.
- (14) (a) Ebbesen, T. W.; Lezec, H. J.; Ghaemi, H. F.; Thio, T.; Wolff, P. A. *Nature* **1998**, *391*, 667. (b) Grupp, D. E.; Lezec, H. J.; Thio, T.; Ebbesen, T. W. *Adv. Mater.* **1999**, *11*, 860. (c) Martín-Moreno, L.; Garcia-Vidal, F. J.; Lezec, H. J.; Pellerin, K. M.; Thio, T.; Pendry, J. B.; Ebbesen, T. W. *Phys. Rev. Lett.* **2001**, *86*, 1114. (d) Salomon, L.; Gillot, F.; Zayats, A. V.; de Fornel, F. *Phys. Rev. Lett.* **2001**, *86*, 1110.